Hindawi
Shock and Vibration
Volume 2020, Article ID 6074658, 13 pages
https://doi.org/10.1155/2020/6074658

Research Article

Experimental Study on City Road Collapse under Vibrating Load

Yuxiao Wang, Gang Shi, Xiaowei Tian, Chaoyue Li, and Huanyu Cheng

School of Civil Engineering, Zhengzhou University, Zhengzhou, Henan 450001, China

Correspondence should be addressed to Yuxiao Wang; 252551297@qq.com

Received 17 August 2019; Revised 30 October 2019; Accepted 15 November 2019; Published 27 January 2020

Academic Editor: Zhixiong Li

Underground pipeline seepage and traffic load are the important factors causing city road collapse. In this paper, eight groups of indoor scale model experiments are used to study the road collapse caused by pipeline seepage, taking into account the load type, pipeline buried depth, the distance between pipeline and loss channel, the relative position of pipeline and loss channel, and the formation time of loss channel. The results show that when the erosion channel was formed later, the underlying erosion cavity was ellipsoid, while the other erosion cavities were funnel shaped. When only the static load is applied, the time to reach the ultimate failure is longer than that when only dynamic load is applied. The smaller dynamic load can increase the stability of the soil above the seepage pipeline, while the larger dynamic load can accelerate the collapse process. With the formation time of the erosion channel increasing, the erosion void size is larger and the surface is easier to collapse. With the increase of the distance between the loss passage and the pipeline, the damage time of the road surface is also increased. The larger the thickness of the soil layer above the pipeline, the smaller the size of the underground cavity and the surface subsidence.

1. Introduction

In recent years, city road collapse accidents occur frequently, bringing huge property losses to people, seriously threatening personal safety. Road collapse and pipeline seepage have a close relationship. There is "Nine Seepage of Ten Collapse." When the pipeline seeps, the soil obtains a certain hydraulic gradient and the soil around the pipeline softens under the erosion of water. Under the action of erosion and scour, the surrounding soil particles are constantly taken away by the flow of water, which makes it easy to form the loss channel. When too many soil particles which include sandy soil and silt generally are washed away, the underlying cavity is formed, thus causing the road surface to lose stability. Roads also play an important role in collapse. The load above the soil tunnel is transferred to the soil layer through the road structure to increase the additional stress of the soil. When the collapse force is greater than the bearing capacity of the roof of the soil cave, the upper soil collapses.

The study of collapse mechanism can be traced back to the 19th century, when the famous Russian geologist Bablov put forward the "erosion theory," which holds that groundwater activity is the main factor causing karst collapse. Ouyang et al. [1] studied the inducement, cavity formation, and expansion of roads collapse and analyzed the mechanical mechanism of the cavity formation. It is pointed out that the formation and expansion of the soil cave are mainly caused by the peeling force. The results show that road collapse mainly undergoes three processes: the formation of voids, the expansion, and the failure of overlying soil. The change of groundwater level is the main reason for the formation of peeling force and plays a decisive role in the formation and expansion of voids. Wang et al. [2] proposed a model for predicting road collapse based on catastrophe theory and analyzed the influence of geological conditions, tunnel buried depth, span, unsupported length, and other factors on road collapse. The results revealed that the surface of the ground is more likely to collapse when the adjacent tunnel is constructed.

Li [3] studied the failure modes of subsidence in coarse-grained and soft soils, analyzed the causes of subsidence, and put forward the calculation formulas of the safety factor of

subsidence for soft soils and coarse-grained soils, respectively. The rationality of the formula is verified by the numerical simulation method. The subsequent analysis suggested that the seepage of groundwater can cause the change of soil strength and pressure difference inside and outside the hole, and it is an important factor to induce subsidence. Sun [4] developed an experimental equipment which can simulate different karst fissures, analyzed the collapse law of different width of karst fissures, and gave the critical width of fissures: when the compactness of silty clay was 1.86 g/cm and 1.90 g/m , the critical crack width was 3 mm and 4 mm, respectively.

Jiang et al. [5] simulated the evolution of karst caves through laboratory-scale experiments and found that the damage of karst soil cave in the vertical infiltration zone mainly occurs at the top, which is mainly due to the infiltration of rain water in the upper part. Yu [6] studied the soil cavities with different shapes by the plane strain experiment, simplified the shape of soil cavities into an ellipse, compared and analyzed the whole process of unstable failure by changing the size of major and minor axis, overburden ratio, inclination angle, and other factors, and summarized the influence of different shapes of cavities on the failure of strata. The results show that the larger the axial length of the horizontal direction of the underlying cavity is, the easier it is to collapse.

Aiming at the problem of damage and leakage of the underground pipeline, Zhang et al. [7] studied the influence of the seepage of water supply pipelines on the surface subsidence during the disturbance of tunnel construction by means of an indoor model experiment. They pointed out that the leakage range is the main factor directly affecting the range of ground collapse and the intensity of formation failure. Rutsch et al. [8] established a test model to analyze the mechanism of drainage pipeline exosmosis, put forward a method to study the seepage rate of the drainage pipeline by using Darcy's law, and obtained several main influencing factors of leakage: height of water head in the leaks, size of leakage mouth, and permeability coefficient of the permeable layer.

Guo [9] put forward a calculation model of pipeline seepage for pressurized and nonpressurized pipelines, evaluated the influence of the permeability coefficient and breakage opening on seepage, and studied the influence of breakage opening size and different water pressure and particle size on soil failure through experiments. The result shows that there is no linear relationship between the damaged area of the pipeline and the leakage. For example, when the radius is 0.1 m and the buried depth is 1 m, if the area of the broken port is doubled, the leakage will increase by about 10%. Liu et al. [10] made use of model experiments to detect the seepage of pipelines and give the recommended values of pipeline seepage parameters under the conditions of buried soil and unburied soil, which are 1.80×10^{-4} and 2.19×10^{-4}, respectively.

In addition, many scholars have made field tests [11, 12] and considered that the properties of soil around the pipeline are an important factor affecting the leakage of the pipeline.

At present, there are still some deficiencies in the research of city road collapse: most scholars pay more attention to the effect of cave on collapse than to the factor of pipeline seepage. When simulating the cavity, the cavity is assumed to be an ideal shape and not representative. In the study of city road subsidence, few scholars have analyzed the influence of dynamic load which can lead to pore pressure rising and destroy the internal structure of soil on road subsidence when pipeline seepage factors exist. In this paper, aiming at the problem of city road subsidence caused by pipeline seepage, the process of road subsidence under dynamic load is studied by the indoor scale experiment. The influence of load type, buried depth of pipeline, distance between pipeline and drain channel, relative position of pipeline and drain channel, and formation time of drain channel on the stability of overlying soil layer is analyzed.

2. Design of Indoor Experimental Plan

2.1. Similarity Ratio Design. The geometric similarity ratio of the model is 1 : 20 due to the limitation of the test site and the loading device. Some of the parameters are selected according to reference [6, 13, 14] and similarity criterion. The remaining parameters can be derived from the similarity ratio principle formula. In the end, we can get the geometric similarity ratio $C_L = 20$, the time similarity ratio $C_t = 20^{1/2}$, the load frequency similarity ratio $C_f = 20^{-1/2}$, the head height similarity ratio $C_H = 20$, the deformation similarity ratio $C_\delta = 20$, the geometric dimension similarity ratio $C_L = 20$, and the other similarity ratios are 1.

2.2. Model Experiment Equipment. The model experiment equipment is composed of four parts: model box system, loading system, pipeline seepage system, and monitoring system.

2.2.1. Model Box. The dimensions of the experiment model box are 1500 mm × 500 mm × 1000 mm (length × width × height), and the geometric similarity ratio is 1 : 20. The steel used in the model box is model Q345. Thickness is 5 mm. Yield strength is 345 MPa. Elastic modulus is 206 GPa. The front of the model box is made of transparent armoured glass whose thickness is 10 mm, and the other four sides are made of steel plate welding. In order to prevent the deformation of the model box and toughened glass during the test, the reinforced steel skeleton is welded around the model box, as shown in Figure 1(a). In practice, the corresponding geometric dimensions of the experiment model box are about 30 m × 10 m × 20 m. There are 10 holes with a diameter of 50 mm in the glass panel. The model box is shown in Figure 2.

2.2.2. Loading System. The loading module is used to simulate the road traffic load. The experiment mainly considers the formation and development process of soil cave and does not consider the interaction between soil and rigid pavement. Therefore, no rigid pavement structure is set in the test.

Traffic load can be composed of two parts: (1) static load, pedestrian and vehicle gravity and other factors; (2) dynamic

Figure 1: Experimental devices. (a) Model box. (b) Vibration exciter. (c) Water tank. (d) PVC pipe. (e) Video recorder. (f) Camera.

load, caused by the impact load of the vehicle motion and other factors. According to the research results of [15], the traffic load is simplified as a simple form of load and the expression is

$$P(t) = P_0 + P_d \sin(\omega t), \quad (1)$$

where $P(t)$ is the applied load, P_0 is the initial static load, P_d is the dynamic load amplitude, ω is the angular frequency, and t is the time.

According to reference [13], it can be seen that when the speed is 80 km/h, the actual pavement loading time is 0.37 s. According to the principle of similarity ratio, it can be calculated that the loading time in the test is 0.062 s, so the loading frequency of the test is 16 Hz. The selection of dynamic load and static load is also based on reference [13], which points out that the vertical stress of the subgrade top surface under driving load is generally between 4 and 8 kPa and the actual situation. So in the test, the static load of 4 kPa is selected and the maximum amplitude of dynamic load is 2 kPa.

In the test, the static load is provided by the weight and the dynamic load is provided by the vibration exciter. The selected vibration exciter model is YZD-2-6, as shown in Figure 1(b). The working principle is as follows: the three-phase 380 V asynchronous vibration motor can obtain the excitation force by using the centrifugal force produced by the high-speed rotation of the shaft and eccentric block. The maximum excitation force is 2 kN, and the maximum rotating speed is 1000 R/min. The excitation force and rotating

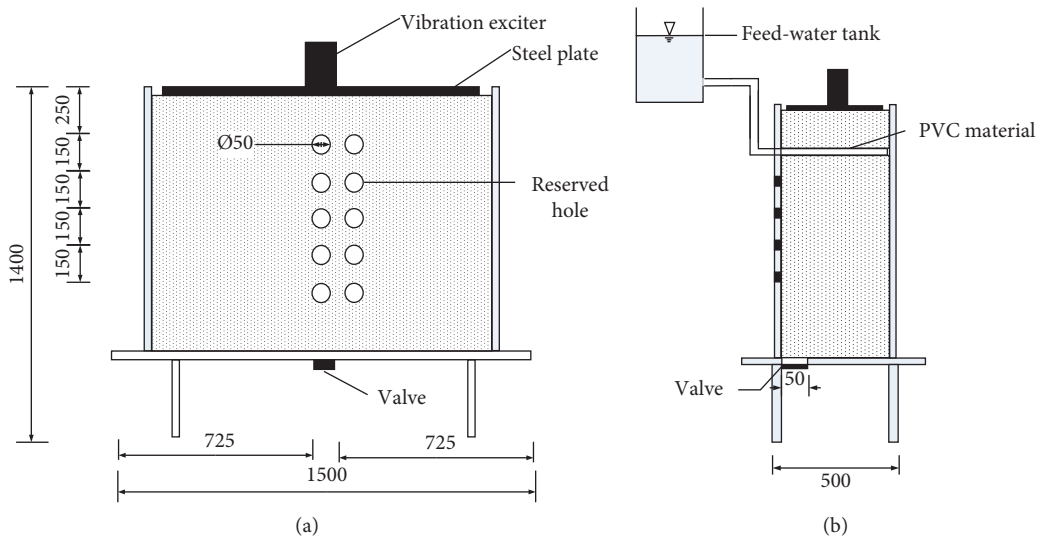

Figure 2: Schematic diagram of the model box. (a) Front view of the model box. (b) Side view of the model box.

speed can be adjusted. The exciter can simulate sinusoidal vibration.

In order to distribute the load evenly on the soil surface, this test adopts the form of the steel plate connected with the exciter. The exciter is located in the positive center of the steel plate and is fixed to each other by bolts as shown in Figure 2(b). The exciter distributes the load evenly on the soil surface through the steel plate. The size of the steel plate used is 140 cm × 40 cm × 1 cm.

2.2.3. Pipeline Seepage Module. The seepage module is composed of a water tank as shown in Figure 1(c) and a PVC pipe as shown in Figure 1(d). The top surface of the PVC pipe has small holes, used to simulate pipeline seepage. Tanks are placed at different heights to simulate different osmotic pressures.

2.2.4. Monitoring System. During the experiment, the progressive failure process of soil mass was photographed by a video recorder as shown in Figure 1(e). At a certain interval, a high-resolution digital camera is used to take pictures, as shown in Figure 1(f) and the picture is post-processed by the Digital Image Correlation software to output the settlement of soil surface from the software.

2.3. Design of Experimental Plan. This paper mainly considers the influence of load type and size (static load P_0 + static load P_0), pipeline buried depth (h), distance between pipeline and lower drain passageway (a), relative horizontal position of pipeline (l), and opening time of valve in the evolution of road collapse failure. The meaning of some parameters is shown in Figure 3. There are 8 conditions in total. The specific scheme of the model is as given in Table 1. A PVC pipe with a diameter of 50 mm is embed in the soil layer, and small holes are arranged on the top surface of the pipe in the soil body to simulate the seepage of the pipeline.

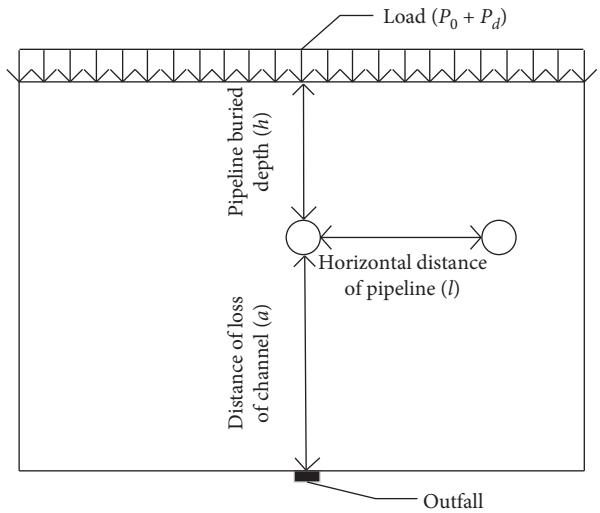

Figure 3: Schematic diagram of the model experiment.

For the selection of model boxes in this test refer to reference [6, 14]. The surface perpendicular to the pipeline can be regarded as the main orientation of soil failure, while the direction along the pipeline is a secondary parameter which does not have too much influence on the test results. In addition, with the limited test conditions, the plane strain model is selected.

3. Description of Experiment Process and Phenomenon

This chapter describes the evolution process of soil failure caused by pipeline seepage under various conditions and combines with the experimental pictures of soil evolution under Condition 2 (static load + dynamic load). The ultimate failure pattern at the end of the experiment under each condition is shown in Figure 4.

Table 1: Model experimental plan of formation instability failure caused by pipeline seepage.

Conditions	Static load P_0 (kN)	Dynamic load P_d (kN)	Pipeline buried depth h (cm)	Distance from lower drain passageway a (cm)	Relative position of pipelines l (cm)	Drain channel open time
1	4	0	15	30	0 from center axis	Experiment initiation
2	4	1	15	30	0 from center axis	Experiment initiation
3	4	1	15	15	0 from center axis	Experiment initiation
4	4	0.5	15	15	0 from center axis	Experiment initiation
5	4	0.5	15	30	0 from center axis	Experiment initiation
6	4	0.5	30	30	0 from center axis	Experiment initiation
7	4	0.5	30	30	15 cm to the right of the center axis	Experiment initiation
8	4	0.5	30	30	0 from center axis	After 320 mins of experimenting

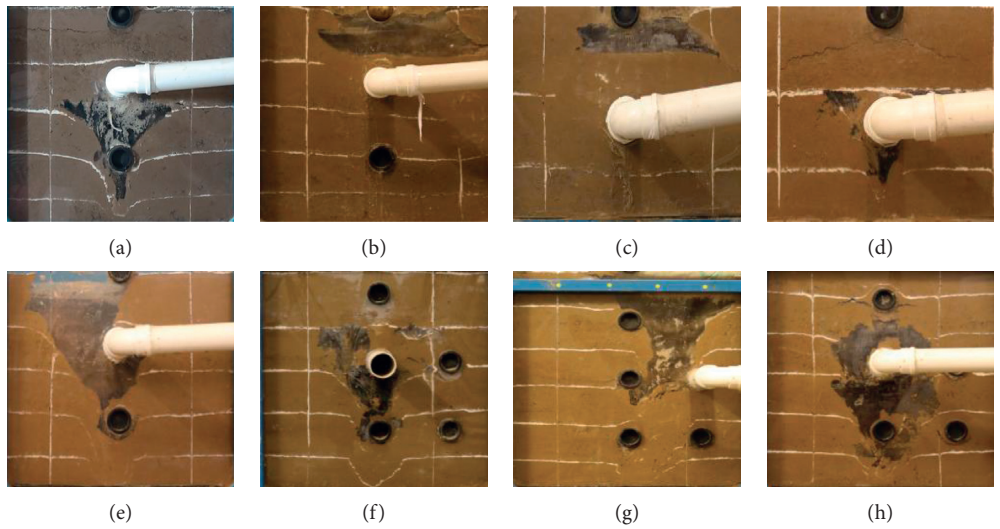

Figure 4: Final failure pattern. (a) Condition 1. (b) Condition 2. (c) Condition 2. (d) Condition 4. (e) Condition 5. (f) Condition 6. (g) Condition 7. (h) Condition 8.

The experiment process and phenomenon of each condition are described as follows:

(1) Condition 1 is the case of static load acting alone. In the experiment, when the water valve was opened for 45 min, the water leaked down 23 cm from the position of the pipeline. At 55 min, it leaked to the bottom of the model box. With the downward seepage of water, transverse cracks gradually appeared in the lower part of the pipeline and there was a trend of continuous transverse propagation. At 120 min, the cracks underneath the pipeline developed symmetrically at 45° and the horizontal distance was about 26.5 cm. At 123 min, the flowing soil appeared. At 131 min, the cavity began to accumulate water, and at 173 min, the cavity formed the ultimate failure shape and the experiment was finished. The final damage is shown in Figure 4(a).

(2) Condition 2 considers the interaction between the static load and the dynamic load. The liquefaction process of soil caused by seepage water at different time is as shown in Figure 5. Therefore, when the experiment was carried out for 40 min, the vertical seepage distance reached 17.5 cm, and at this time, 7.5 cm transverse cracks appeared directly below the pipeline. When the experiment was carried out for 50 min, the vertical permeation had already reached the bottom of the tank. At 65 min, the transverse crack continued to develop to 11 cm and the right side of the crack began to expand downwards. When the time was 100 min, the transverse crack reached 15 cm and there was water accumulation near the pipeline. At 125 min, the transverse cracks spread to 21 cm because of the existence of vibration load, the soil above the pipeline began to fall off, and the height of cracks increased and spread upward. When

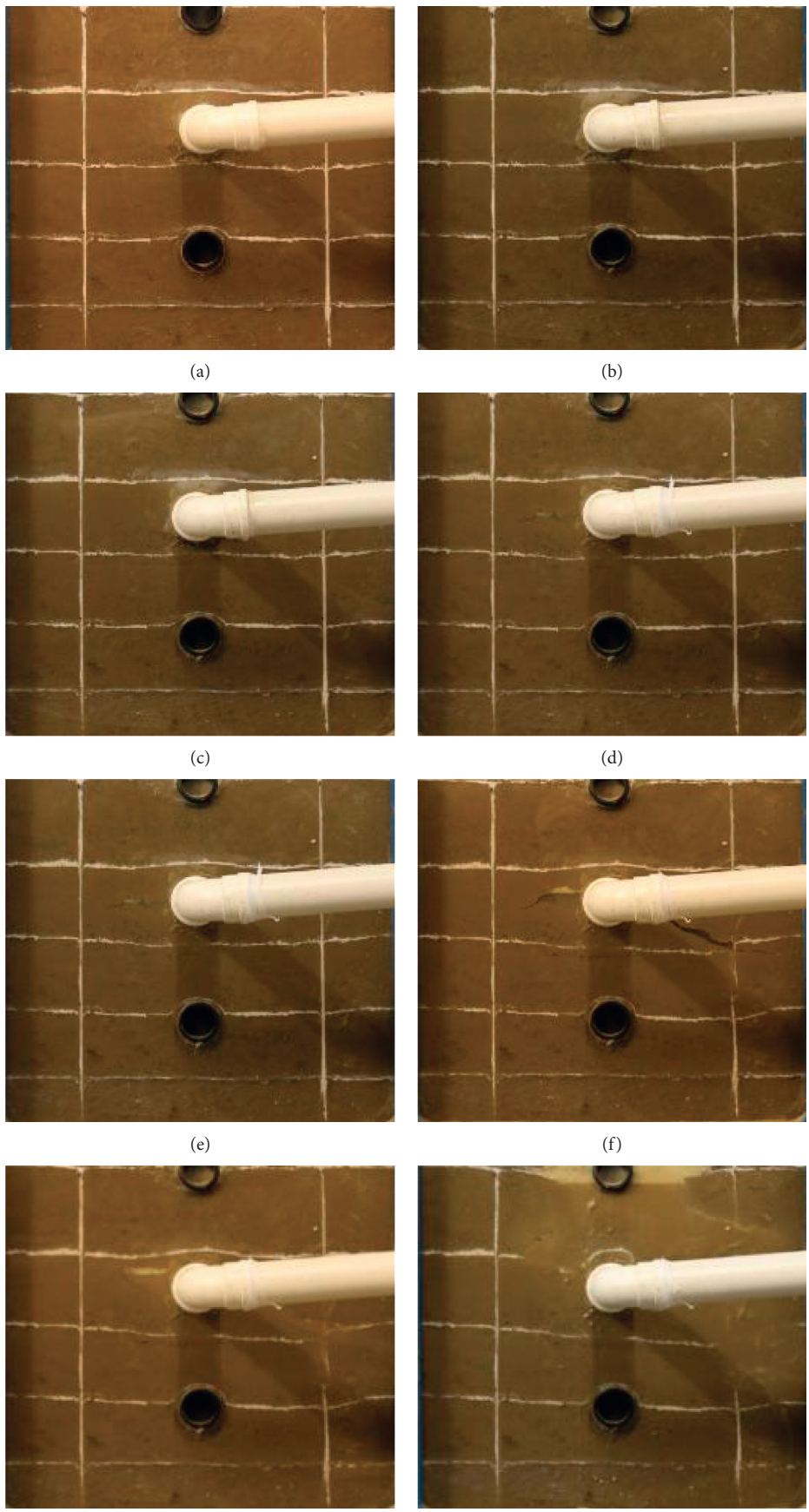

Figure 5: Experiment phenomenon of Condition 2. (a) 0 min. (b) 40 min. (c) 65 min. (d) 100 min. (e) 125 min. (f) 160 min. (g) 184 min. (h) 200 min.

the experiment was carried out for 160 min, the highest crack position coincided with the uppermost part of the pipeline. At 184 min, the crack in the upper part of the pipeline began to extend rapidly upward. Finally, at 200 min, the soil was finally destroyed, the experiment was finished, and the ultimate failure pattern is as shown in Figure 4(b).

Combined with the experimental phenomenon of working Condition 2, the damage of soil will be explained microscopically: when the underground pipeline was damaged, the surrounding soil structure will be destroyed due to the hydrostatic pressure and dynamic water pressure. Because there are pores in the middle of the soil particle skeleton, water can flow through these pores, and when the water flows, it will act on the surface of the soil particles with a certain force f^0, which can be decomposed into vertical direction f_x^0 (hydrostatic pressure direction) and parallel to the soil particle surface direction f_y^0 (dynamic water pressure direction). When f_x^0 or f_y^0 is greater than the shear strength of the pipeline failure, the soil particles will peel off, with the seepage direction moving and taking it to the distant pore, and then the pore around the pipeline will expand. When these pores are connected together, there will appear obvious cracks. According to the experimental phenomenon, the cracks in the soil first appear directly above the leakage. The cracks in the soil are not only the temporary shelter of the collapsed soil, but also the channel of soil particle transfer. The seepage field increases with the increase of cracks and accelerates the latent erosion of surrounding soils. With the increase of leakage, the cracks will continue to expand to form a cavity zone. When the cracks extend down to a certain extent, the loss channel will be penetrated, the seepage speed will be faster, and the soil particles will be peeled off faster. According to the test phenomenon, when the cavity area develops to a certain size, a large soil mass collapse can be observed and the collapsed soil falls at the bottom of the empty area and gradually transfers down with the leakage. When the size of the cavity area develops to a certain extent, the soil cave finally collapses.

(3) Condition 3 is the case where both h and a are on the small side. When the experiment was carried out for 20 min, a 12.5 cm long void area was formed around the pipeline and the void area was filled with water. At 60 min, the overlying soil began to collapse. Finally, at 70 min, the cracks penetrated the soil surface to reach the ultimate failure and the experiment was finished. The ultimate failure pattern is shown in Figure 4(c).

(4) Condition 4 is the case in which h, a, and the dynamic load are small. When the water valve was opened for 1 min, cracks will appear under the pipeline. At 25 min, the soil above the pipeline began to be damaged by tension and shear. At 40 min, the flowing soil appeared below and the ultimate failure form was formed at 42 min, and the experiment was finished. The final destruction is shown in Figure 4(d).

(5) Condition 5 is the case that a is larger than that of Condition 4. At the beginning of the experiment, the soil was soaked down 23 cm. At 52 min, water had penetrated to the bottom of the model tank. At 160 min, a vertical crack with a length of about 2.3 cm appeared on the right side of the model box at a distance of about 40 cm from the center (as shown in Figure 6). 163 min later, the flowing soil appeared. At 165 min, transverse tensile cracks appeared above the pipeline. At 190 min, the vacant area developed rapidly downwards and on both sides, and finally destroyed at 220 min. The ultimate failure pattern is shown in Figure 4(e).

(6) Condition 6 is the case with large h compared with Condition 5. At the beginning of 70 min, the water infiltrated to the bottom of the model box and transverse cracks appeared in the flush position around the pipeline, without longitudinal cracks. Longitudinal cracks appeared at 110 min. At 125 min, the flowing soil appeared, and after a few min, the longitudinal cracks expanded rapidly, forming a relatively large void area and the void area was filled with water. At 290 min, the loss channel penetrated the soil and reached the ultimate failure form. The ultimate failure pattern is shown in Figure 4(f).

(7) The main characteristic of Condition 7 is that the distance between loss channel and pipeline is 15 cm. The lateral distance between the drain passage and the pipeline passage is 15 cm. At 55 min, water penetrates to the bottom of the model tank and the maximum lateral range of lateral infiltration is 48 cm. At 135 min, flow soil appeared and no void appeared before 140 min, but transverse cracks were observed in the upper soil and the surface subsidence was obvious. Then, within 20 min, the void zone rapidly developed to 45° on the upper side of the pipeline, with a length of 10.5 cm. After 255 min, the liquid in the void zone eroded the soil on the upper and lower sides and formed an ultimate failure pattern through the void zone. The ultimate failure pattern is shown in Figure 4(g).

(8) Under Condition 8, the drain channel was closed first and then opened. When the lower loss channel did not exist, the infiltration range increased with the increase of the water flow rate. At 320 min, soak into the whole soil, then the lower valve was opened and the soil flowed out a few min later and the development rate of the emptying zone was much faster than that of the other groups. Finally, at 425 min, the upper soil collapsed, blocking the loss channel, and the experiment was finished, and the ultimate failure form is as shown in Figure 4(h).

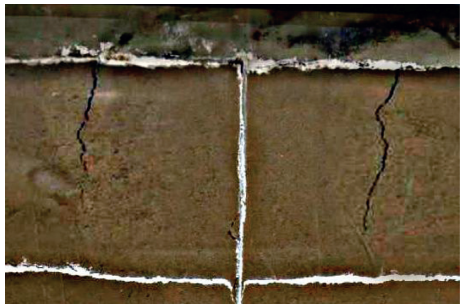

Figure 6: Vertical cracks.

4. Comparative Analysis of Model Experiment Results

4.1. Influence of Load Type and Size. The failure process of soil under static and dynamic loads is studied under Conditions 1–5, respectively. Condition 2 and 3 stop the test when the void area extends to the surface, and in practice, the final cavity size will be larger than the existing test results and the longitudinal penetration will run from the surface to the bottom of the model box. The transverse width of the underground cavity formed in working Condition 5 is small, mainly because of uneven compaction or other reasons in the process of filling, and the transverse width should be larger in the actual process.

4.1.1. To Form a Hollow Contrast. Experiment 1 formed voids on the underside of the pipeline. Experiments 2 and 3 formed voids above the pipeline. The cavity formed in Experiment 4 was higher than the pipeline at the top. The voids formed in Experiment 5 run through the whole model. The void parameters are shown in Table 2.

As can be seen from Table 2, the time taken to form the final failure form from Model Test 1 to Model Test 5 is 173 minutes, 220 minutes, 77 minutes, 42 minutes, and 200 minutes, respectively. Combined with Table 2 and the failure process of soil, it can be obtained as follows.

The main results are as follows:

(1) The failure time is reduced when only static loads act on the surface of the soil, than when the static and dynamic load act together.

(2) When the dynamic load is small, the time to reach failure increases less. When the dynamic load is moderate, the time to reach failure increases more. If the dynamic load is too large, the failure of soil will be accelerated.

(3) On the basis of single static load, increasing dynamic load will increase the area of failure area. Although it will delay the failure time under certain conditions, it will increase the degree of failure.

The analysis suggests that when the dynamic load is small, the vibration can increase the compactness of the soil, so the soil is not easy to destroy. To sum up, appropriately increasing the dynamic load value can increase the stability of soil and delay the time of pavement failure.

4.1.2. Comparison of Land Subsidence Trough. The noncontact measuring equipment is used to get information of settlement. The center point of the settlement trough refers to the point in the middle of the soil surface, as shown in Figure 7.

At the end of the experiment, the comparison diagram of the settlement tank is shown in Figure 6. By comparing only static load (Condition 1) and static and dynamic load acting at the same time (Conditions 2 and 5), the settlement value of the center point of the latter is larger, which indicates that the dynamic load will increase the settlement of the soil under certain conditions. Comparing with Conditions 2 and 5, it can be found that the settlement value increases when the dynamic load is reduced by half, which is due to the limitation of the conditions in Condition 2, and the experiment can be stopped when the hole extends to the surface, so the maximum settlement value decreases instead, and the settlement value will increase if it is consistent with the actual situation.

At the end of the experiment, the comparison diagram of the settlement tank is shown in Figure 8. By comparing only static load (Condition 1) and static and dynamic load acting at the same time (Conditions 2 and 5), the settlement value of the center point of the latter is larger, which indicates that the dynamic load will increase the settlement of the soil under certain conditions. Comparing with Conditions 2 and 5, it can be found that the settlement value increases when the dynamic load is reduced by half, which is due to the limitation of the conditions in Condition 2, and the experiment can be stopped when the hole extends to the surface, so the maximum settlement value decreases instead, and the settlement value will increase if it is consistent with the actual situation.

Combined with working Conditions 2, 3, 4, and 5, the following conclusion is obtained: the settlement will be more than doubled when the distance of the lost channel is doubled.

In Conditions 3 and 4 (larger h/a), the settlement ratio of the overlying soil layer to the pipeline is 4 and 5 (smaller h/a). This indicates that when the h/a is large, the stability of the underground cavity is better and the settlement is small.

4.1.3. Comparison of Soil Evolution. Only under static load, the void zone extends downwards from the bottom of the pipeline as shown in Figure 9(a). When the dynamic and static loads act simultaneously, the void zone extends horizontally from the middle of the pipeline and then extends downwards to a certain extent.

In addition, the transverse tensile cracks are easy to appear in the overlying soil layer under static load only as shown in Figure 10. If the dynamic load is added to the foundation, the tensile cracks are difficult to appear. It is because the dynamic load has a vibrocompaction effect on the soil. But the area of the damaged area will be enlarged, when the dynamic load is present, and when large voids appear in the soil, the soil tends to slip to both sides, so vertical tensile cracks as shown in Figure 5 are easy to occur.

Table 2: Comparison table of soil cavity parameters.

Condition	Hollow shape	Forming time (min)	Horizontal maximum width (cm)	Longitudinal height (cm)
1	Half funnel	173	29	27.5
2	Cuboid	220	34.5	8.8
3	Cuboid	77	25	7.2
4	Half funnel	42	22	21
5	Half funnel	200	21.3	45

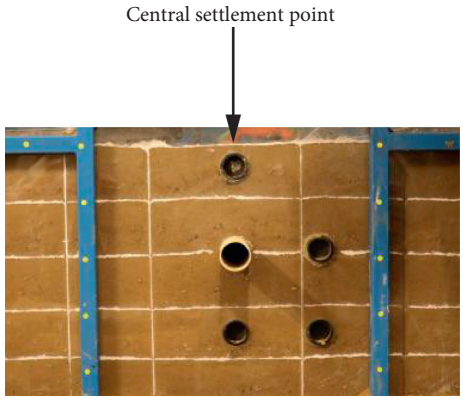

Figure 7: Central settlement point.

4.2. Effect of Distance between Loss Channel and Seepage Pipeline. The influence of the distance between the loss passage and the seepage pipeline was studied under Conditions 4 and 5. The experiment results, in Figure 7, are compared as follows.

4.2.1. Comparison of Soil Voids. Unlike Condition 5, the cavity in Condition 4 penetrates from the upper part of the pipeline to the bottom of the model box and does not extend to the surface. The characteristics of the soil cavity formed in the two groups of experiments are shown in Table 3.

From the point of view of formation time, the distance between pipeline and loss channel is reduced by 50% and the formation time of final failure form is reduced by about 80%, which indicates that the distance between different pipeline and loss channel has a great influence on the formation time of the final failure form. From the point of view of the size of the cavity although the horizontal width of the two pairs is not much different, the longitudinal height of Condition 4 is more than twice that of Condition 5, which indicates that when the distance between the pipeline and the lost channel is large, the degree of surface collapse is greater.

4.2.2. Comparison of Surface Settlement. As shown in Figure 11, the settlement value of the ground surface under Condition 4 and Condition 5 is very small. In Condition $h/a = 1$, Condition $h/a = 0.5$, and Condition 4, the settlement value is more stable. In Condition 5, the thickness of the overlying soil layer is half of the distance between the loss channels and the cavity is closer to the ground surface, so the settlement value is larger. The analysis shows that when h/a is larger, the drain channel is often longer. When the flow passes through the channel, the resistance is too large and the dynamic water pressure cannot be effectively released, so there is a large water pressure near the leakage pipeline, so the water scour the soil around the pipeline more violently and the settlement increases. This is consistent with Section 4.1.

4.2.3. Comparison of Soil Evolution. There is no vertical tensile crack in Condition 4, and only one arch crack does not extend to the surface. In Condition 5, the vertical tensile crack appears in the soil on both sides of the cavity and the soil tends to collapse in the middle. Description: the larger the h/a, the smaller the probability of extending to the surface for the void area, and the vertical tensile crack is not easy to appear on both sides of the void area.

On the whole, the larger the ratio of the buried depth of pipeline to the distance between pipeline and loss channel is, the more stable the overlying soil layer is.

4.3. Influence Analysis of Thickness of Overlying Soil Layer on Seepage Pipeline. The influence of pipeline depth on foundation instability is studied and compared in Conditions 5 and 6.

4.3.1. Comparison of Soil Voids. With the increase of the pipeline buried depth, the failure time of soil cavitation is gradually increased. It is analyzed that with the increase of the thickness of the soil layer above the pipeline, if the soil collapses, the area of its fracture will increase and its ability to resist failure will increase. Therefore, with the increase of the thickness of the soil layer above the pipeline, the underground cavity is more stable and the upper soil is difficult to be destroyed, so the failure time is reduced. The horizontal crack lengths formed in Conditions 5 and 6 are 21.3 cm and 21 cm, respectively. The holes in Condition 5 extend to the surface, but not in Condition 6. It can be seen from the analysis that the hole size will decrease and the stability will increase with the increase of the buried depth of the pipeline. See Table 4 for the hole parameters.

4.3.2. Comparison of Surface Settlement. According Figure 12, when the buried depth is doubled, the settlement decreases by about 30%. The settling value of Condition 5 is larger than that of Condition 6, which indicates that the thicker the overlying soil layer is, the smaller the settling amount is. In the sixth experiment condition, there is neither vertical crack nor transverse crack, which indicates that the stability of road can be increased by increasing the buried depth of pipeline.

In general, the greater the thickness of the overlying soil layer on the pipeline is, the more stable is the road surface.

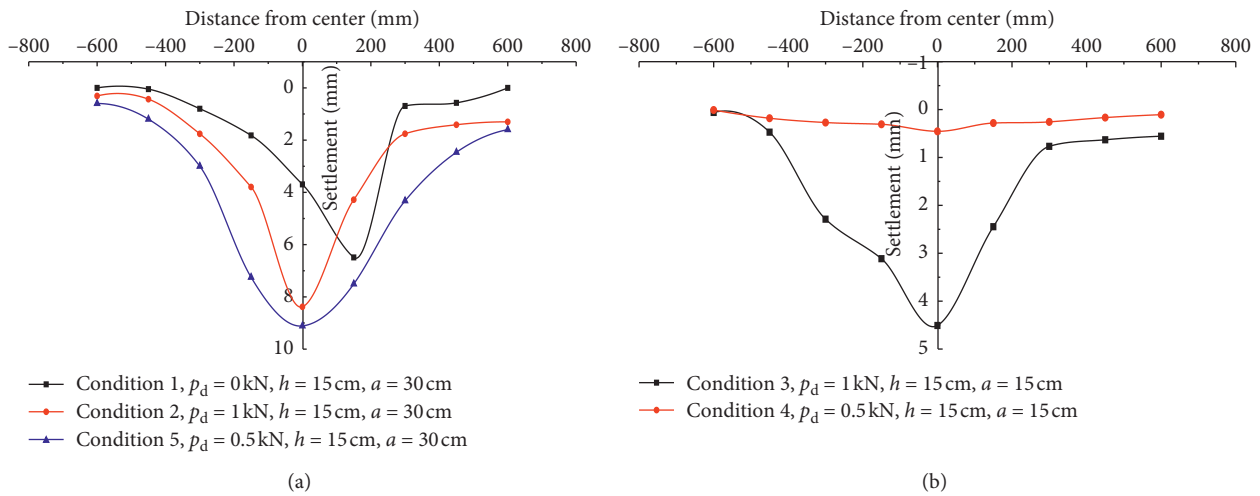

Figure 8: Influence of load type and size on settlement tank. (a) ($h/a = 0.5$). (b) ($h/a = 1$).

Figure 9: The development of void zone. (a) Condition 1. (b) Condition 2. (c) Condition 3. (d) Condition 4. (e) Condition 5.

4.4. Influence Analysis of Relative Position of Loss Channel and Seepage Pipeline. The influence of the relative position of the loss passage and the seepage pipeline is compared under Conditions 6 ($l = 0$) and 7 ($l = 15$ cm).

The void parameters are shown in Table 5. The time of Condition 6 is longer than that of Condition 7, and the final horizontal width of cavity formation is larger than that of Condition 6, but the shape of cavity formation is almost the

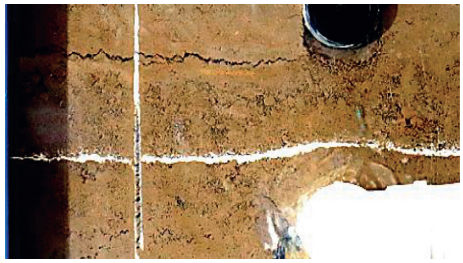

Figure 10: The transverse tensile crack.

Table 3: Experiment 4 and 5 cavity parameter table.

Experiment group	Hollow shape	Forming time (min)	Horizontal maximum width (cm)	Longitudinal height (cm)
4	Half funnel	42	22	21
5	Half funnel	200	23	45

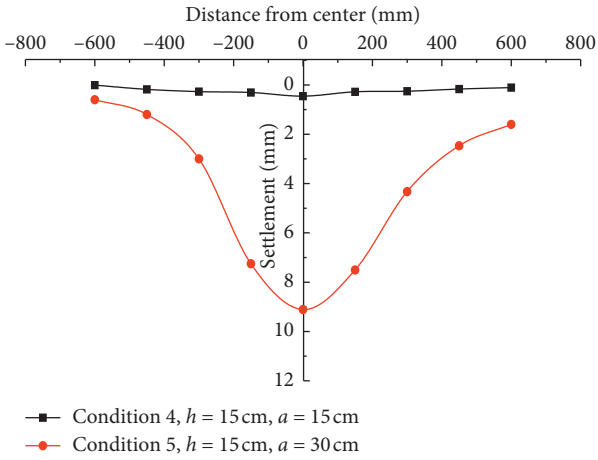

Figure 11: Effect of distance between loss channel and pipeline on settlement tank.

Table 4: Experiment 4 and 5 cavity parameter.

Condition group	Hollow shape	Destroyed time (min)	Horizontal maximum width (cm)	Longitudinal height (cm)
5	Half funnel	220	21.3	45
6	Half funnel	290	21	40

same. As shown in Figure 13, the contrast diagram of the settling tank shows that the infiltration range of Condition 7 is larger and the settlement is larger and the settlement on the right side of Condition 7 is obviously larger than that on the left side. Unlike the other groups, the emptying zone under Condition 7 does not develop horizontally, but obliquely upwards and also tends to develop towards the lower drain passage, but develops slowly. The analysis shows

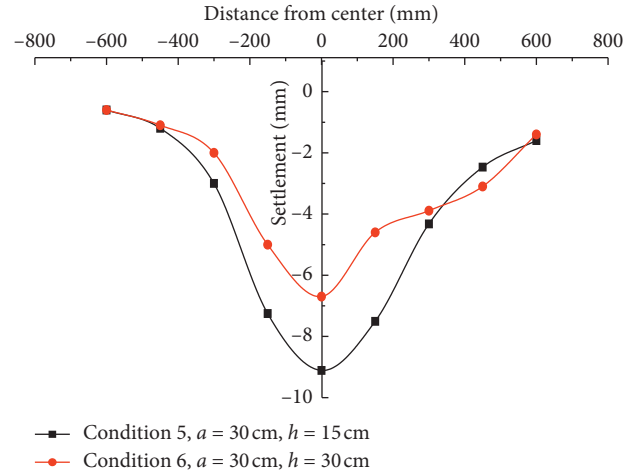

Figure 12: Influence of the thickness of the overlying soil layer on the settlement tank of the pipeline.

Table 5: Experiment 4 and 5 cavity parameter table.

Experiment group	Hollow shape	Forming time (min)	Horizontal maximum width (cm)	Longitudinal height (cm)
6	Half funnel	180	21	40
7	Half funnel	255	36	60

that with the pipeline moving to the right, the distance between the loss channel and the pipeline increases and the resistance of the development of the void area increases, which will increase the rate of upward development and increase the size of voids and extend the final damage time.

4.5. Influence Analysis of Formation Time of Loss Channels. Condition 8 opens the drain valve later than Condition 6.

4.5.1. Comparison of Soil Voids. As shown in Table 6, the cavity formed in Condition 6 is larger than that in Condition 8 and the infiltration rate and area in Condition 6 are faster and bigger than those in Condition 8. The analysis shows that the larger the infiltration range is, the larger the cavity is. This is because the leakage of water has a certain effect on the failure of formation instability. On the one hand, it will weaken the deformation modulus and strength of the soil. On the other hand, it will also increase the deadweight load of soil, so it will aggravate the deformation and failure of soil.

4.5.2. Comparison of Surface Settlement. The contrast diagram of the settling tank is shown in Figure 14. The channel of the settling tank under Condition 6 is opened all the time, and the channel of the settling tank under Condition 8 is opened only when the infiltration range is very large in 320 min, and the settling value of the latter is larger, indicating that under the same condition, the sooner the drain channel is opened, the more stable the cavity is. If the loss

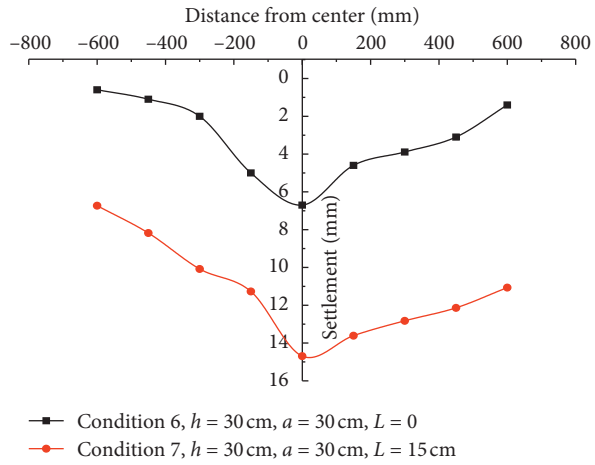

Figure 13: Effect of phase position of loss channel and pipeline.

Table 6: Experiment 6 and 8 cavity parameter Table 6.

Experiment group	Hollow shape	Forming time (min)	Horizontal maximum width (cm)	Longitudinal height (cm)
6	Half funnel	180	21	40
8	Half funnel	435	23	42

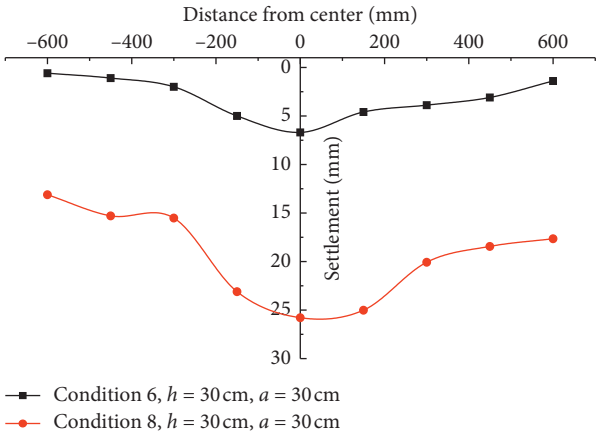

Figure 14: Effect of formation time of loss channel on settlement tank.

channel does not exist, the seepage water of the pipeline will only diffuse in the soil, and if there is vibration load in the upper part, there will be dense effect. In this case, only settlement will occur and no void area will appear. If the loss channel is opened in the state that the soil has been soaked to a great extent, the void area will develop very quickly and the surface will collapse easily.

4.5.3. Comparative Analysis of the Evolution of Soil. After the lost channel is opened, the water and soil mixture flows out of the lower loss channel and the empty area is developed from the center of the pipeline towards the horizontal and the vertical direction. The lost channel is opened at the beginning in Condition 6, the seepage leakage is mainly extended downwards, and the upward expansion speed is slow, so the soil body on the upper side of the pipeline is relatively stable; however, when the whole soil body range is wetted, the lost channel is opened (Condition 8). At this time, the soil on the upper side of the pipeline is completely wetted, the strength is reduced, the empty area is more likely to expand upwards, and the surface is easy to collapse.

5. Conclusion

In this paper, the indoor scale model experiment is adopted and the factors such as load type, pipeline buried depth, distance between pipeline and loss channel, relative position of pipeline and loss channel, and formation time of loss channel are taken into account. The problem of road collapse caused by pipeline seepage is studied. The conclusions are as follows:

(1) When the erosion channel is formed late, the underlying erosion cavity is ellipsoid, while the erosion cavity is funnel-shaped under other conditions. The range of soil infiltration is proportional to the formation time of loss channel.

(2) When only static load is applied, the time to reach the ultimate failure is longer than that when only dynamic load is applied and tensile cracks are more likely to occur in the upper part of the pipeline. When the dynamic load is present, the area of the damaged area will be enlarged. When the dynamic load is small, the stability of the soil above the seepage pipeline is increased. When the dynamic load is large, the development speed of the void area is accelerated and the collapse is more likely to occur.

(3) With the formation time of the loss channel increasing, the length of the seepage channel substantially increases, the stability of the soil above the pipeline decreases, the erosion is easier to reach the surface, and the collapse is easier to occur. When the distance between the loss passage and the pipeline increases, the time of ultimate damage will also increase. When the relative position of the loss channel and the pipeline changes, the surface subsidence on one side of the loss channel is larger and the ultimate failure mode is located on this side.

(4) The larger the ratio of the thickness of the overlying soil layer and the lost channel is, the more stable the soil is. Under the combined action of static load and dynamic load, the settlement of the soil before failure decreases by about 30% when the buried depth of the soil is doubled. When the length of the lost channel is doubled, the settlement before the failure of the soil will be more than double.

Data Availability

All data used to support the findings of this study are available from the corresponding author upon request.

Conflicts of Interest

The authors declare that they have no conflicts of interest.

References

[1] Z. H. Ouyang, M. F. Feng, and C. H. Li, "Study on formation and expansion mechanism of hidden soil cavity in ground collapse," *Metal Mine*, vol. 6, pp. 16–19, 2006.

[2] C. P. Wang, S. Meng, and D. L. Zhang, "Prediction model for ground collapse induced by urban tunnelling," *China Railway Science*, vol. 33, no. 4, pp. 31–37, 2012.

[3] T. Li, Z. Z. Zong, and Z. L. Dan, "Study of formation mechanism and prediction of sinkholes in soil stratum induced by subterranean cavity," *Rock and Soil Mechanics*, vol. 36, no. 7, pp. 1995–2002, 2015.

[4] J. H. Sun, *Study on Critical Parameter in Cover Karst Collapse by Model Experiment and Numerical Simulation*, Southwest Jiaotong University, Chengdu, China.

[5] X. J. Jiang, M. T. Lei, and Z. D. Guan, "Formation mechanism of karst soilvo- id in single-layer soil structure condition," *Carsologica Sinica*, vol. 31, no. 4, pp. 426–432, 2012.

[6] L. Yu, *Test Study on Failure Mechanism of Underground C-Avity in Different Forms in Urban Strata*, Beijing Jiaotong University, Beijing, China, 2013.

[7] C. Zhang, Y. Yue, and M. Wang, "Influence of pipeline leakage on ground collapse and its control during adjacent tunnelling," *China Civil Engineering Journal*, vol. S1, pp. 351–356, 2015.

[8] M. Rutsch, J. Rieckermann, and P. Krebs, "Quantification of sewer leakage: a review," *Water Science and Technology*, vol. 54, no. 6-7, pp. 135–144, 2006.

[9] S. Guo, *Study on Infiltration and Soil Erosion in Sewer Systems*, Zhejiang University, Hangzhou, China, 2012.

[10] W. Liu, L. N. Huang, and J. Li, "Experiment on leakage of water pipelines," *Journal of Earth-Quake Engineering and Engineering Vibration*, vol. 31, no. 4, pp. 167–173, 2011.

[11] A. Sawangsuriya, A. Jotisankasa, and S. Anuvechsirikiat, *Classification of Shrinkage and Swelling Potential of a Subgrade Soil in Central Thailand*, Springer, Berlin, Germany, 2012.

[12] C. J. Rogers, *Sewer Deterioration Studies: The Background to the Structural Assessment Procedure in the Sewerage Rehabilitation Manual*, Water Research Centre, Wales, UK, 1986.

[13] J. M. Ling, W. Wang, and H. B. Wu, "On re sidual deformation of saturated clay subgrade under vehicle load," *Journal of Tongji University*, vol. 30, no. 11, pp. 1315–1320, 2002.

[14] S. C. Wang, *Analysis and Study on Subsidence Mechanisms of Road Caused by Leakage of Urban Underground Pipeline*, Zhengzhou University, Zhengzhou, China, 2017.

[15] F. Tian and J. J. Zhu, "Research on traffic load characteristics and simulation methods," *Journal of Water Resources and Architectural Engineering*, vol. 12, no. 4, pp. 66–161, 2014.